7 • Strontium isotope stratigraphy

J. M. MCARTHUR AND R. J. HOWARTH

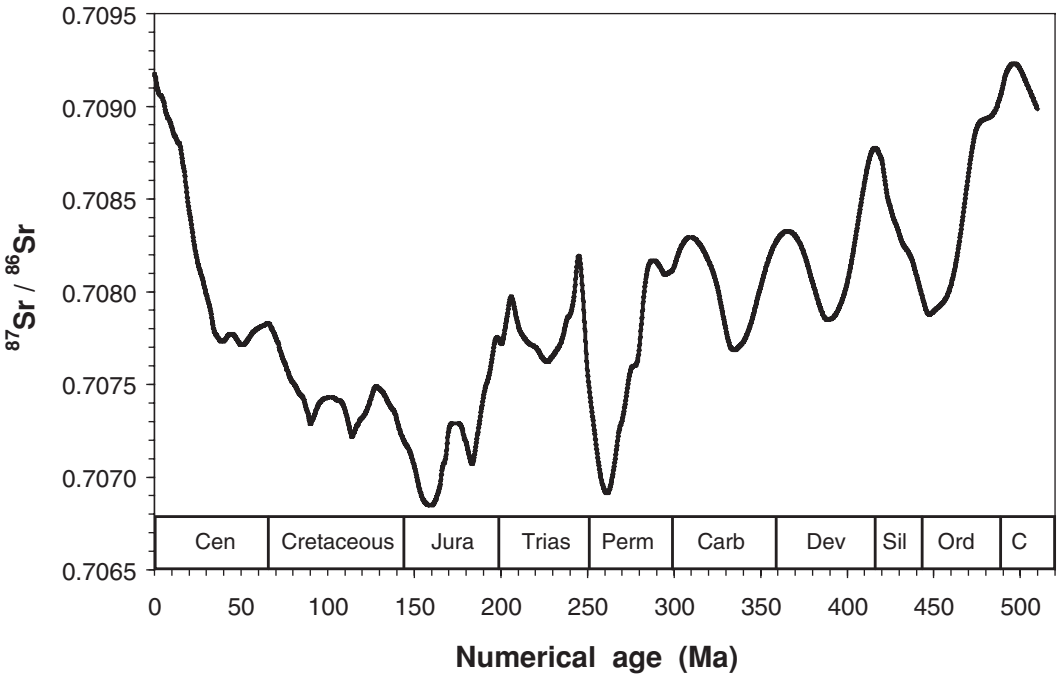

Figure 7.1 Variation of $^{87}Sr/^{86}Sr$ through Phanerozoic time. LOWESS fit to data sources in Table7.1.

The $^{87}Sr/^{86}Sr$ value of Sr dissolved in the world's oceans has varied though time, which allows one to date and correlate sediments. This variation and its stratigraphic resolution is discussed and graphically displayed.

7.1 INTRODUCTION

The ability to date and correlate sediments using Sr isotopes relies on the fact that the $^{87}Sr/^{86}Sr$ value of Sr dissolved in the world's oceans has varied though time. In Fig. 7.1, we show this variation, plotted according to the time scale presented in this volume. More detail is given in Fig. 7.2, on which we plot both the curve of $^{87}Sr/^{86}Sr$ through time and the data used to derive it. Comparison of the measured $^{87}Sr/^{86}Sr$ of Sr in a marine mineral with a detailed curve of $^{87}Sr/^{86}Sr$ through time can yield a numerical age for the mineral. Alternatively, $^{87}Sr/^{86}Sr$ can be used to correlate between stratigraphic sections and sequences by comparison of the $^{87}Sr/^{86}Sr$ values in minerals from each (Fig. 7.3). Such correlation does not require a detailed knowledge of the trend through time of $^{87}Sr/^{86}Sr$, but it is useful to know the general trend in order to avoid possible confusion in correlation near turning points on the Sr curve.

Strontium isotope stratigraphy (SIS) can be used to estimate the duration of stratigraphic gaps (Miller *et al.*, 1988), estimate the duration of biozones (McArthur *et al.*, 1993, 2000, 2004) and stages (Weedon and Jenkyns, 1999), and to distinguish marine from non-marine environments (Schmitz *et al.*, 1991; Poyato-Ariza *et al.*, 1998). The degree to which such things can be accomplished rests, in part, on how well the trend in marine $^{87}Sr/^{86}Sr$ through time can be defined, and it is this issue that concerns us here. For a more detailed account of SIS, the reader is referred to reviews by McArthur (1994) and Veizer *et al.* (1997, 1999).

A Geologic Time Scale 2004, eds. Felix M. Gradstein, James G. Ogg, and Alan G. Smith. Published by Cambridge University Press.

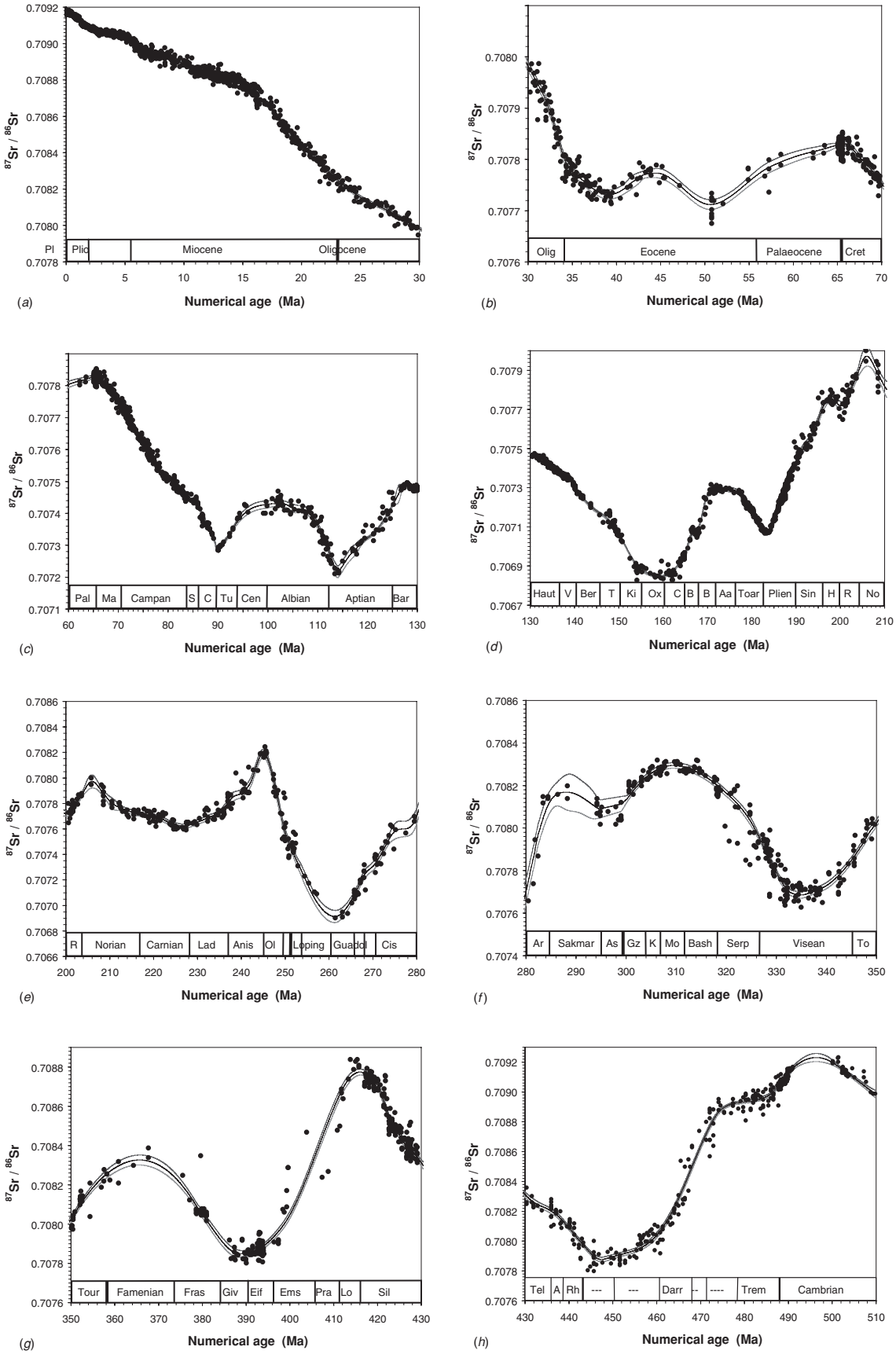

Figure 7.2 Details of the variation of $^{87}Sr/^{86}Sr$ through time given in Fig. 7.1, showing width of 95% confidence intervals. See text for a discussion of its parts.

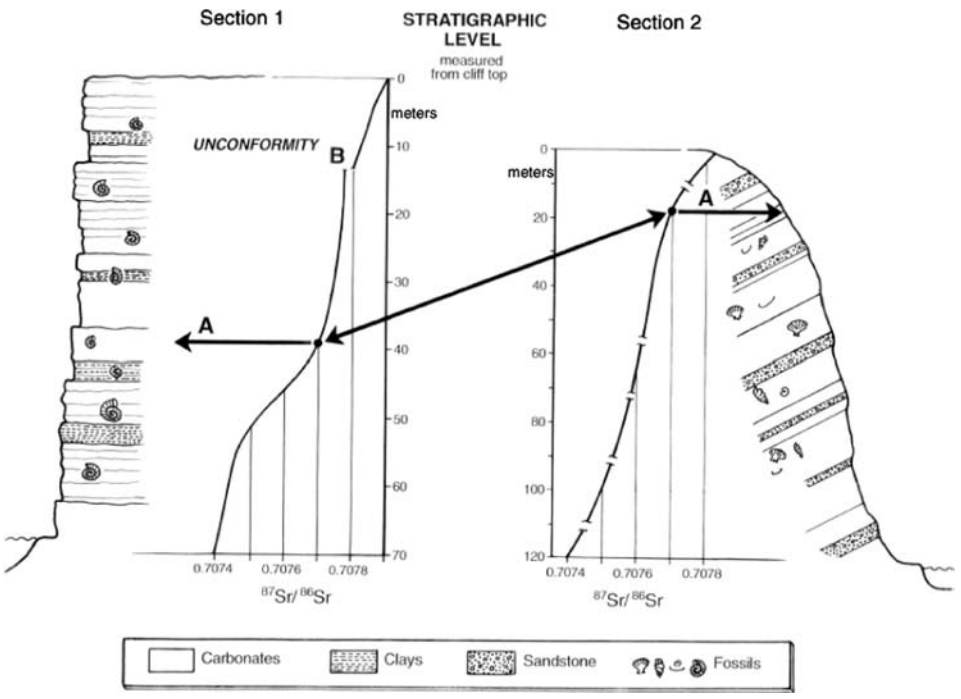

Figure 7.3 Correlation with $^{87}Sr/^{86}Sr$. Values of $^{87}Sr/^{86}Sr$ are matched between $^{87}Sr/^{86}Sr$ profiles constructed for independent sections.

The method works only for marine minerals. Practitioners assume that the oceans are homogenous with respect to $^{87}Sr/^{86}Sr$ and always were so. Uniformity of $^{87}Sr/^{86}Sr$ is expected for two reasons. First, because the residence time of Sr in the oceans ($\approx 10^6$ years) is far longer than the time it takes currents to mix the oceans ($\approx 10^3$ years), so the oceans are thoroughly mixed on time scales that are short relative to the rates of gain and loss of Sr. Second, because the amount of Sr in the sea (7.6 μg/l) is much greater than the amount in rivers (variable, but two orders of magnitude less), the effect of riverine dilution is small; seawater maintains a $^{87}Sr/^{86}Sr$ value that is characteristic of the open ocean until it is diluted to salinities well below those supportive of fully marine fauna (Andersson *et al.*, 1992). Tests of the homogeneity of $^{87}Sr/^{86}Sr$ in modern open oceans and some restricted seas (DePaolo and Ingram, 1985; Andersson *et al.*, 1992; Paytan *et al.*, 1993) confirm that it appears to be homogenous at an analytical precision of ±0.000 020. Since those studies were done, the precision of measurement of $^{87}Sr/^{86}Sr$ has improved to around ±0.000 003 for replicate determinations, so the assumption of uniformity now requires re-evaluation.

7.2 MATERIALS FOR STRONTIUM ISOTOPE STRATIGRAPHY

Of the materials that have been used for SIS, belemnite guards (Jones *et al.*, 1994a,b; McArthur *et al.*, 2000) and brachiopod shells (Veizer *et al.*, 1999) have proven useful, since they resist diagenetic alteration better than other forms of biogenic calcite. Early diagenetic marine carbonate cements have made an important, if volumetrically minor, contribution to SIS calibration in the lower Phanerozoic (Carpenter *et al.*, 1991). Foraminiferal calcite, largely from DSDP/ODP sites, has yielded the curve for the Neogene (see works of Farrell and others, Hodell and others, Miller and others; Table 7.1), while acid-leached, nannofossil-carbonate ooze (McArthur *et al.*, 1993), inoceramids (Bralower *et al.*, 1997), atoll carbonates (Jenkyns *et al.*, 1995), and ammonoid aragonite (McArthur *et al.*, 1994) have all yielded useful data. Attempts to use barite have met with mixed success (Paytan *et al.*, 1993; Martin *et al.*, 1995; Mearon *et al.*, 2003). The use of conodonts seems to work for samples with a color-alteration index of around 1, which implies minimal alteration (Martin and Macdougall, 1995; Ruppel *et al.*, 1996; Ebneth *et al.*, 2001; Korte *et al.*, 2003).

7.3 *A GEOLOGIC TIME SCALE 2004* (GTS2004) DATABASE

The standard curve of $^{87}Sr/^{86}Sr$ as a function of time presented here (Figs. 7.1 and 7.2, and available in a supplementary tabulation from the authors: j.mcarthur@ucl.ac.uk) is updated from that given in McArthur *et al.* (2001) and uses 3875 data pairs from the sources listed in Table 7.1. This table also gives

Table 7.1 *Sources of data used for the LOWESS fit*

Author	Normalizer ($\times 10^6$)	Age range (Ma)	
Azmy *et al.* (1999)	30	417	443
Banner and Kaufman (1994)	−3	337	342
Barrera *et al.* (1997): Site 463; new age model	13	67.7	74.5
Bertram *et al.* (1992): conodonts	11	420	435
Bralower *et al.* (1997): inoceramids	0	94.7	116.3
Brand and Brenckle (2001): some	0	319	319
Bruckschen *et al.* (1999)	30	325	359
Callomon and Dietl (2000)	0	164.2	164.4
Carpenter *et al.* (1991)	3	379	380
Clemens *et al.* (1993, 1995)	−6	0.0	0.2
Cummins and Elderfield (1994): brachiopods	11	327	331
Denison *et al.* (1993)	102	45.6	65.3
Denison *et al.* (1994)	102	257	360
Denison *et al.* (1997)	102	364	438
Denison *et al.* (1998)	102	445	510
DePaolo and Ingram (1985): Palaeogene	−59	38.1	65.65
Diener *et al.* (1996): brachiopods	30	378	400
Ebneth *et al.* (2001): Texas and Australia	33	487.5	491
M. Engkilde, *pers. comm.* (1998)	0	144.2	175.9
Farrell *et al.* (1995): pruned 2.8–3.5 Ma	−9	0.0	7.0
Henderson *et al.* (1994)	17	0.0	0.37
Hodell *et al.* (1991): Holes 588 and 588A	18	7.3	18.3
Hodell and Woodruff (1994): new age model	18	10.9	23.3
Jenkyns *et al.* (1995)	−12	99.7	125.2
Jones *et al.* (1994a,b): some	22	100.8	199.7
Koepnick *et al.* (1990)	102	201	251
Korte *et al.* (2003)	25	200	252
Martin and Macdougall (1995)	−12	248	295
Martin *et al.* (1999): <13.8 Ma	22	5.0	13.8
McArthur *et al.* (1993)	0	71.1	89.1
McArthur *et al.* (1993)	0	69.4	84.3
McArthur *et al.* (1994)	0	71.4	99.1
McArthur *et al.* (1998)	0	65.4	68.1
McArthur *et al.* (2000)	0	177.1	189.6
McArthur and Kennedy (unpub. data)	0	96.0	107.8
McArthur and Morton (2000)	0	170.8	174.2
McArthur *et al.* (in review)	0	2.6	3.6
McArthur *et al.* (2004)	0	124.2	133.4
McArthur and Janssen (unpub. data)	0	133.6	138.4
Mead and Hodell (1995)	18	18.6	45.3
Miller *et al.* (1988)	−14	22.9	33.7
Miller *et al.* (1991)	−14	9.1	24.1
Montañez *et al.* (1996)	−6	500	505
Oslick *et al.* (1994): >16 Ma	−14	16.0	25.0
Qing *et al.* (1998): <463 Ma	5	420	489
Ruppel *et al.* (1996)	−7	417	442
Sugarman *et al.* (1995)	−14	65.7	72.4
Zachos *et al.* (1992, 1999)	0	23.2	42.2

the amount added to, or subtracted from, the literature data in order to correct for apparent inter-laboratory bias in measurement of $^{87}Sr/^{86}Sr$. Such bias is assumed to represent systematic error and to be correctable by such a normalization process. As replication of $^{87}Sr/^{86}Sr$ measurement can give mean values precise to ±0.000 003 (Jones *et al.*, 1994a; McArthur *et al.*, 2001), inter-laboratory bias must be quantified to this precision if SIS is to realize its full potential.

We correct data to a common value of 0.710 248 for standard reference material NIST-987 (formerly known as SRM-987) or a value of 0.709 175 for EN-1, a modern *Tridachna* clam from Enewetak Atoll (prepared by the USGS). Some older work is normalized to a $SrCO_3$ standard, known as "E and A," that was prepared by the Eimer and Amend company (New York; now owned by Fisher Chemical). The $^{87}Sr/^{86}Sr$ value of E and A is 0.708 022 ± 4 (2 s.e., $n = 34$) relative to a value for NIST-987 of 0.710 248 (Jones *et al.*, 1994a). In a few cases, our normalizer is based on evaluation of inter-laboratory bias that is independent of the published source of data, so it may be different from that given in the source.

7.3.1 Numerical ages

The revised SIS calibration curve given here (Figs. 7.1 and 7.2) uses the GTS2004 time scale of this volume. Where original data were reported to other time scales, the original ages have been converted to the current time scale using the formulae of Wei (1994) and the nearest pair of numerically dated stratigraphic tie points. In some instances, where local or regional stratigraphy has advanced since the publication of a source, we have revised the age models used in original publications.

The calibration curve shown in Figs. 7.1 and 7.2 is based on measurement of $^{87}Sr/^{86}Sr$ in samples dated by biostratigraphy, magnetostratigraphy, and astrochronology (mostly the first two). The difficulty of assigning numerical ages to sedimentary rocks by the first two methods is well known. Users of the calibration curve, and the equivalent look-up tables derived from it that enable rapid conversion of $^{87}Sr/^{86}Sr$ to age and vice versa (McArthur *et al.*, 2001), must recognize that the original numerical ages on which the curve is based may include uncertainties derived from interpolation, extrapolation, and indirect stratigraphic correlations and may suffer from problems of boundary recognition (both bio- and magnetostratigraphic), diachroneity, and assumptions concerning sedimentation rate, all of which contribute uncertainly to the age models used to generate the calibration line. Furthermore, age models are ultimately based (mostly) on radiometric dates and are as accurate as those dates. Interpolation of ages between tie points, however, may be more precise, although necessarily systematically inaccurate.

7.3.2 Fitting the database

We used the statistical non-parametric regression method LOWESS (LOcally WEighted Scatterplot Smoother of Cleveland, 1979, 1981; Chambers *et al.*, 1983; Thisted, 1988; Cleveland *et al.*, 1992) to obtain a best-fit curve for the $^{87}Sr/^{86}Sr$ data as a function of time. Details of the fitting procedure are given in Howarth and McArthur (1997). Because of the complex shape of the fit, and the very uneven density of data points through time, the curve was optimized by being fitted in 29 overlapping local segments. These were then joined using splines at segment junctions. To obtain a table for predicting age from $^{87}Sr/^{86}Sr$, and the lower and upper confidence limits on the age, we used inverse interpolation of the fitted curve of $^{87}Sr/^{86}Sr$ and its 95% confidence intervals (CIs) as a function of age. The complete table is available from j.mcarthur@ucl.ac.uk.

7.3.3 The quality of the fit

CONFIDENCE LIMITS ON THE LOWESS FIT

In addition to the best-fit curve of estimated $^{87}Sr/^{86}Sr$ as a function of age, the LOWESS fitting process also provides a two-sided, 95% CI, on the estimates of age. These CIs are included in Fig. 7.2, but are best seen in Fig. 7.4 as a half-width interval plotted against time. The width of the CI varies with numerical age, and is dependent on both the density and spread of the calibration data. For substantial segments of the Mesozoic, values approach ±0.000 005 and are seldom more than ±0.000 010. Where data are abundant and samples well preserved, e.g. 0–7 Ma, the half-width CI is around ±0.000 003. Where data are few, e.g. most of the Permian, the uncertainty is much greater. Well-preserved samples become rarer with increasing age so the uncertainty envelope increases with age; nevertheless, achieving a precision of ±0.000 015 for the entire Paleozoic is not an unrealistic goal.

Assuming that the half-widths of the upper and lower confidence intervals are approximately equal, and that U = (upper age CI − estimated age) and L = (estimated age − lower age CI), then the overall uncertainty on an age derived from the curve can be computed by combining the uncertainties on the measurement and the fitted curve as follows:

$$s_{\text{total}} = \left(s_m^2 + s_c^2\right)^{1/2}, \tag{7.1}$$

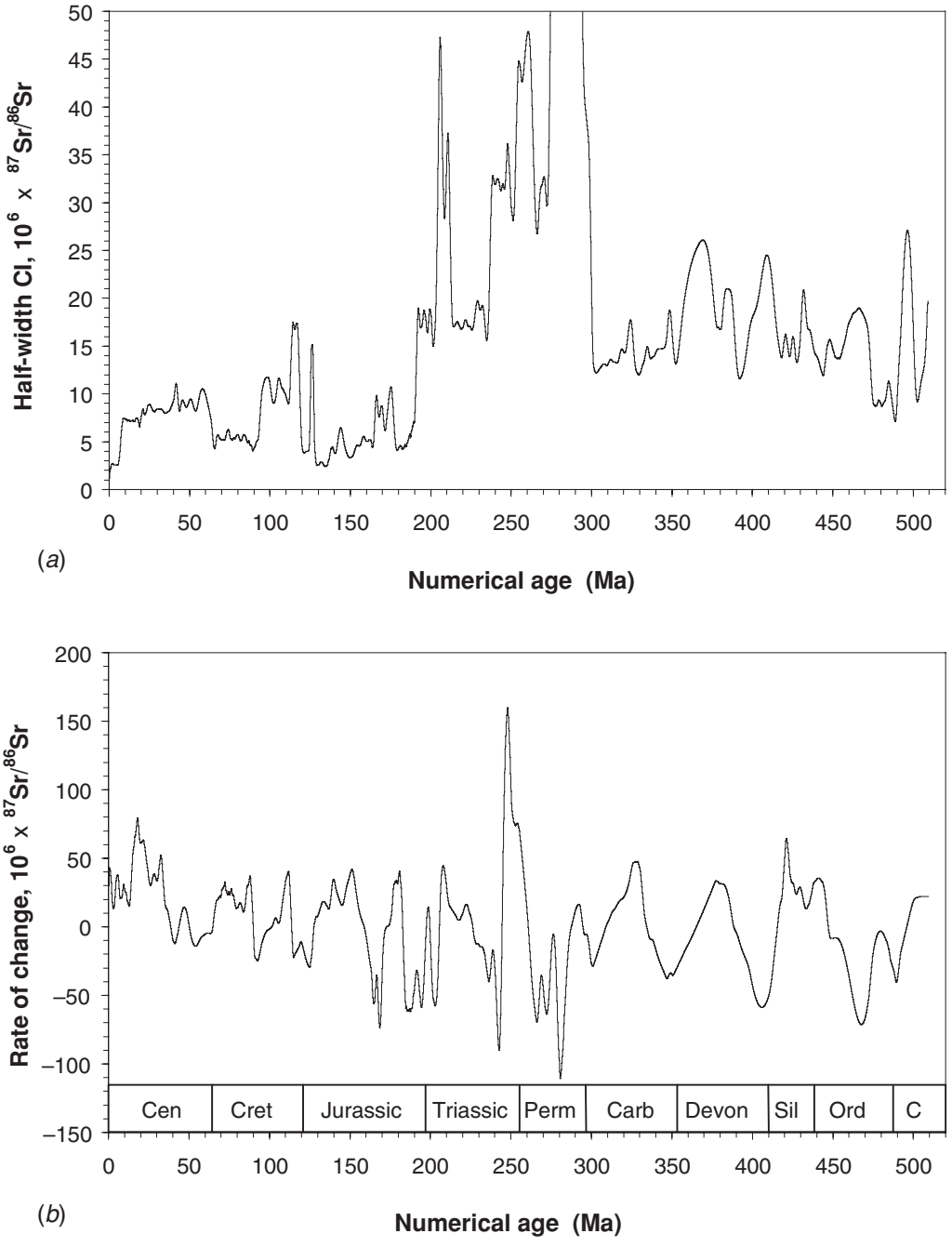

Figure 7.4 (*a*) Half-width of the 95% confidence intervals on the LOWESS fit, and (*b*) rate of change with time of $^{87}Sr/^{86}Sr$.

where s_m is the standard deviation of the estimated numerical age of the sample and $s_c = ((L + U)/2)/1.96$. If L and U are different enough, then it may be preferable to use upper and lower bounds for s_{total} by replacing s_c with L/1.96 and U/1.96, respectively.

Inter-laboratory bias introduces an additional source of uncertainty, since few laboratories have reported precise estimates of the $^{87}Sr/^{86}Sr$ value of their standards, i.e. a comparison of mean $^{87}Sr/^{86}Sr$ in NIST-987 and EN-1, each given to a precision of less than ±0.000 005. The uncertainty from this source can be as high as 0.000 020. As a consequence, inter-laboratory bias may limit the quality of dates and correlations determined using SIS.

CONFIDENCE LIMITS ON MEASURED $^{87}Sr/^{86}Sr$

The uncertainty with which the mean (m) $^{87}Sr/^{86}Sr$ of a sample is known, from n independent determinations of $^{87}Sr/^{86}Sr$,

may be quantified if one assumes that the measurement errors are normally distributed and so a two-sided confidence interval applies:

$$m \pm t_{1-\alpha/2,\ n-1}(s/n^{1/2}), \tag{7.2}$$

where s is the standard deviation of n observed $^{87}Sr/^{86}Sr$ values, and $t_{1-\alpha/2,n-1}$ is the $100(1-\alpha/2)$th percentile of Student's t-statistic with $(n-1)$ degrees of freedom; α is the risk (specified as a proportion) that the true (but unknown) value of $^{87}Sr/^{86}Sr$ in the mineral, which is estimated by m, will fall outside the specified confidence interval. Thus α is commonly set to 0.05 (5%) in order to obtain two-sided 95% confidence limits on m. The t-statistic is used for this purpose rather than the $100(1-\alpha/2)$th percentile of the cumulative normal distribution in order to correct for the fact that the number of replicate determinations of $^{87}Sr/^{86}Sr$ is finite. Increasing n decreases the uncertainty in m. For example, the multipliers for two-sided 95% confidence limits when $n = 2$, 3, 4, 5, and 10 are 12.71, 4.30, 3.18, 2.78, and 2.26, respectively.

It may be possible to obtain only a single determination of $^{87}Sr/^{86}Sr$ (x) for a given mineral sample. If, for some reason, there exists a *prior* estimate of the expected value of $^{87}Sr/^{86}Sr$ (a), e.g. from measurements previously made on presumed similar material, or the ratio has been estimated from the $^{87}Sr/^{86}Sr$ curve and a knowledge of the sample's stratigraphic position, then, assuming x is the centre of a normal distribution, Blachman and Machol (1987) showed that a two-sided $100(1-\alpha)$% confidence interval on x is given by:

$$x \pm (1 + 0.484/\alpha)|x - a|. \tag{7.3}$$

If α is 0.05, the multiplier equals 9.68. Less-conservative bounds are obtained by inverting the prediction interval for a single future observation. This gives:

$$x \pm z_{1-\alpha/2}(1 + 1/n_0)^{1/2}s_0. \tag{7.4}$$

In this case, s_0 is a *prior* estimate of the standard deviation of the distribution (assumed normal) from which x is drawn, e.g. the pooled standard deviation based on n_0 sets of previous determinations of similar samples, and $z_{1-\alpha/2}$ is the $100(1-\alpha/2)$th percentile of the cumulative normal distribution. If α is 0.05, the multiplier equals 1.96.

The best analytical precision on $^{87}Sr/^{86}Sr$ that has so far been obtained by repeated replicate measurements of $^{87}Sr/^{86}Sr$ over a period of time is ±0.000 003 (2 s.e.; Jones *et al.*, 1994a; McArthur *et al.*, 2001). Figure 7.4 shows that little of the global Sr curve has yet been defined to this degree of precision.

NUMERICAL RESOLUTION

The uncertainty of an estimated numerical age obtained using the calibration curve (Figs. 7.1 and 7.2) depends on: (i) the width of the 95% CI on the calibration curve, (ii) the uncertainty with which the $^{87}Sr/^{86}Sr$ of a sample is known, and (iii) the slope of the curve. Given that the best-defined parts of the calibration curve have half-width CIs no better than ±0.000 003, and that this is also the best-attainable precision on measurement of $^{87}Sr/^{86}Sr$, application of (i) above gives a minimum total uncertainty in dating of around 0.000 004. Given that the slope of the calibration curve (Fig. 7.4) rarely exceeds a value of 0.000 060 per myr, it follows that the precision in dating with $^{87}Sr/^{86}Sr$ will not be better than about ±0.1 myr and will generally be much worse. Correlation with $^{87}Sr/^{86}Sr$ avoids the uncertainty involved in assigning numerical ages and the accuracy with which it can be accomplished depends upon: (i) the sedimentation rate of the sequences, or sections, being correlated; (ii) the uncertainty with which the $^{87}Sr/^{86}Sr$ of a sample is known; and (iii) the slope of the curve.

Under optimum conditions, e.g. with well-preserved material and where the rate of change with time of marine $^{87}Sr/^{86}Sr$ is steep, the precision with which SIS can date and/or correlate marine strata can surpass foraminiferal biostratigraphy in the Cenozoic and ammonite biostratigraphy in the Mesozoic. The utility and accuracy of SIS declines as the target rocks get older, since the method relies on analysis of well-preserved samples, mostly biogenic calcite, and these become less common and more likely to be altered as age increases.

RUBIDIUM CONTAMINATION

A further potential problem arises from the fact that samples may contain Rb, the radioactive isotope of which, ^{87}Rb, decays to ^{87}Sr, thereby altering the $^{87}Sr/^{86}Sr$ of even a perfectly preserved sample. The Rb^+ ion is too large, and its marine abundance too low, for it to be found in worrying amounts in biogenic calcite, but the larger cation site in aragonite will accommodate Rb more easily. Rubidium should therefore be monitored in all samples, if the Sr/Rb weight (ppm) ratio is >8000, samples of Phanerozoic age will have altered their $^{87}Sr/^{86}Sr$ by <0.000 003. As a rule of thumb, concentrations of Rb above 0.1 ppm may require a correction to their $^{87}Sr/^{86}Sr$. A table for making such Rb corrections can be found in McArthur (1994).

7.4 COMMENTS ON THE LOWESS FIT

Some details of the GTS2004 database and fit require comment.

Pliocene to now For the period from 0 to 7 Ma, we rely mostly on the data of Farrell *et al.* (1995) excepting between 2.8 and 3.4 Ma. In this interval, these authors' data are too high by up to 0.000 020 and have been pruned and supplemented by $^{87}Sr/^{86}Sr$ data from the astronomically calibrated Pliocene type section at Punta Piccola, Sicily, (McArthur *et al.*, unpub.)

Early Miocene In the LOWESS fit of McArthur *et al.* (2001) the high scatter of data between 22 and 24 Ma was attributed to the effects of diagenetic alteration of the material analyzed. We now believe that explanation to be incorrect and that the scatter results from an uncertain age model for DSDP Site 588C (Hodell *et al.*, 1991), so we no longer use data for 588C; we retain data for Sites 588 and 588A after updating the age models to this time scale. For Site 289 (Hodell and Woodruff, 1994), we use a revised age model that includes breaks in the sequence between 522 and 544 meters below seafloor (mbsf).

Paleogene The $^{87}Sr/^{86}Sr$ curve for the Paleogene shows sufficient slope for it to be potentially useful for dating (Fig. 7.2*b*). From the K–P boundary (65.5 Ma) value of 0.707 83, $^{87}Sr/^{86}Sr$ declines to 0.707 72 in the Ypresian (51Ma) before rising sharply to a maximum of 0.707 78 in the early Lutetian (46 Ma) and then declining again to a second minimum of 0.707 73 in the earliest Bartonian (40 Ma). Thereafter, the ratio increases steeply until modern times. For the Paleocene, the rate of decrease in $^{87}Sr/^{86}Sr$ of around 0.000 08 per myr should give a resolution in dating no better than 0.5 myr, and then only if both curve and $^{87}Sr/^{86}Sr$ measurement of the sample achieve the best-attainable precision. Given that this quality has been achieved in the late Neogene (Farrell *et al.*, 1995), Late Cretaceous (McArthur *et al.*, 1993), early Jurassic (Pliensbachian–Toarcian, McArthur *et al.*, 2000) and Hauterivian times (McArthur *et al.*, 2004), it seems possible to do so.

Maastrichtian For the Late Maastrichtian interval, we use the data of Sugarman *et al.* (1995) and Barrera *et al.* (1997), for DSDP Site 463, the latter after recalibration to the age model of Li and Keller (1999).

Aptian–Albian Of Bralower *et al.*s' (1997) data, we use only that for inoceramids. We have adjusted the Albian boundary ages of Bralower *et al.* (1997) to those in this volume, but retain his apportionment of time between them. The scaling given in this volume distorts the Sr isotope curve in an unreasonable way (cf. Fig. 7.5*a*,*b*), increasing its slope in the basal-Albian,

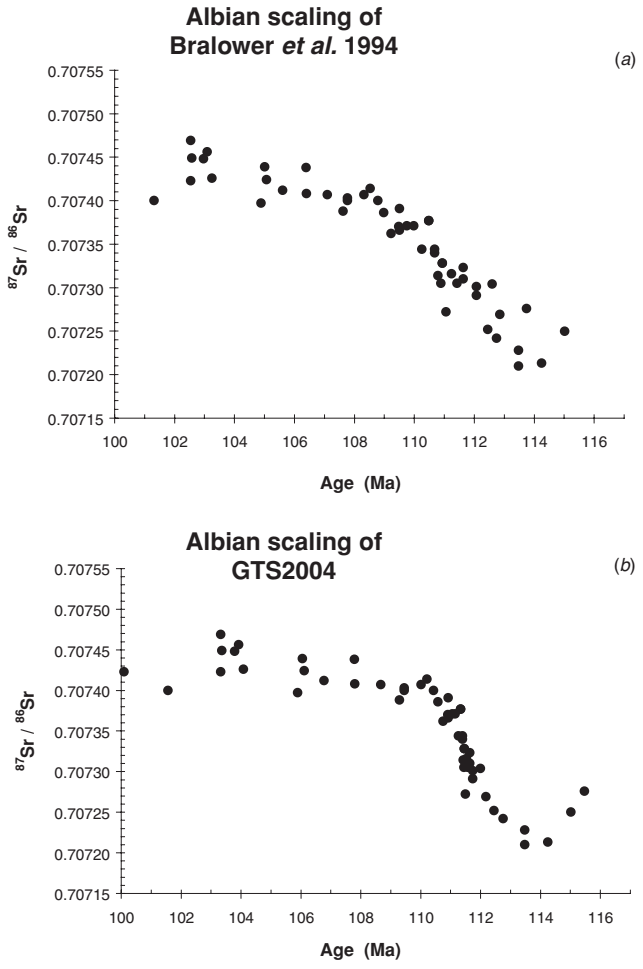

Figure 7.5 Trend in $^{87}Sr/^{86}Sr$ in the Albian–Aptian: data of Bralower *et al.* (1997) for inoceramids plotted against (*a*) the biozonation given by the authors and (*b*) that given in this volume. The age scaling of Bralower *et al.* (1997) is used for the construction of the LOWESS fit.

introducing a break-in-slope at the Aptian–Albian boundary, and stretching data into a plateau above 110 Ma.

Jurassic The data of Jones *et al.* (1994a,b) for the Toarcian, Berriasian, Valanginian, Hauterivian, and Barremian stages are replaced by data in McArthur *et al.* (2000), McArthur *et al.* (2004), and McArthur and Janssen (unpub. data). For the Valanginian and Berriasian, these data have been assigned numerical ages based on equal zone duration, excepting that the uppermost two Valanginian zones (of *Criosarasinella furcillata* and *Neocomites peregrinus*) are allotted a duration that is one half that of other zones. For the Hauterivian and Barremian time, ages are assigned on the basis of a polynomial model that assigns a linear increase of $^{87}Sr/^{86}Sr$ with time through the Hauterivian and lowermost Barremian, and a maxima and

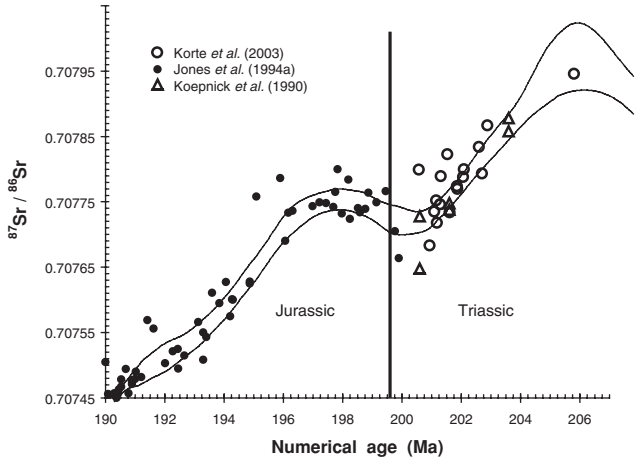

Figure 7.6 Trend in $^{87}Sr/^{86}Sr$ at the Triassic–Jurassic boundary and the accompanying LOWESS fit, showing the 95% confidence intervals on the mean line.

downturn in $^{87}Sr/^{86}Sr$ through the *fissicostatum, elegans*, and *denkmanni* ammonite zones (McArthur *et al.*, 2004).

Triassic Two Rhaetian data are from Jones *et al.* (1994a). The rest are from Koepnick *et al.* (1990) and Korte *et al.* (2003). The peaks in the earliest and latest Triassic are shown in both the second and third sets of data, but as the second data set is based on analysis of whole rocks, and the last (around the peaks) is based on conodonts, which do not preserve their isotope ratios well, the amplitudes of the peaks may be enhanced by artifacts of diagenesis. At the Triassic–Jurassic boundary there is a possible mismatch (Figs. 7.2*d* and 7.6) between the trend of the UK data of Jones *et al.* (1994a), which is calibrated with ammonites, and the trend of the data of Korte *et al.* (2003) and Koepnick *et al.* (1990), which is calibrated with conodonts. The putative mismatch may result from problems of integrating these different biostratigraphic schemes; nevertheless, the two Rhaetian samples of Jones *et al.* (1994a) fall on the Triassic trend of the other authors, so it may be real and we have honored the data in making a fit through this interval (Fig. 7.6). The steepness of the rise in $^{87}Sr/^{86}Sr$ in the very earliest Triassic, and the apparent break-in-slope of the $^{87}Sr/^{86}Sr$ curve at the Permian–Triassic boundary (Fig. 7.2*e*), might be revealing an undue compression of the time scale in the basal Triassic.

Permian The Ochoan data of Denison *et al.* (1994) and the data for the latest Permian given by Martin *et al.* (1995) differ by up to 3.5 myr around the Permian–Triassic boundary. We include both data sets, despite the decrease in precision this causes in the fit, because the differences are certainly caused by problems of age assignment and correlation. As with some Carboniferous data, $^{87}Sr/^{86}Sr$ might here be used to correlate the different sections used by these authors, rather than be composited to form a global curve.

Carboniferous The Carboniferous data rely heavily on that of Bruckschen *et al.* (1999) but those data show a large spread, especially in the Serphukovian and Visean Stages; even after extremes flyers are ignored, values of $^{87}Sr/^{86}Sr$ range from 0.707 637 to 0.707 805 around 332 Ma. Bruckschen *et al.*s' (1999) data from Germany group more tightly than do their data from Belgium, and are mostly higher (by about 0.000 070). The high spread of the data increases the width of the confidence interval in this part of the Carboniferous. The $^{87}Sr/^{86}Sr$ data might be better used to refine correlation, particularly between the USA and Europe, than be used to construct a global standard curve. Finally, much of the data of Denison *et al.* (1994) for the late Carboniferous is some 0.000 100 higher in $^{87}Sr/^{86}Sr$ than data given in Bruckschen *et al.* (1999), so we use only the latter in our fit from 304 to 315 Ma.

Ordovician The trend in $^{87}Sr/^{86}Sr$ across the Cambrian–Ordovician boundary differs markedly between data sets (Fig. 7.7). The least slope is seen in the data of Gao and Land (1991) for the Arbuckle Limestone of Oklahoma. The differences may be caused by incompatible local age models. It is important to determine the trend because different trends necessitate different rates of decline in $^{87}Sr/^{86}Sr$ in the mid Ordovician (*sensu lato*), and the steeper ones having been

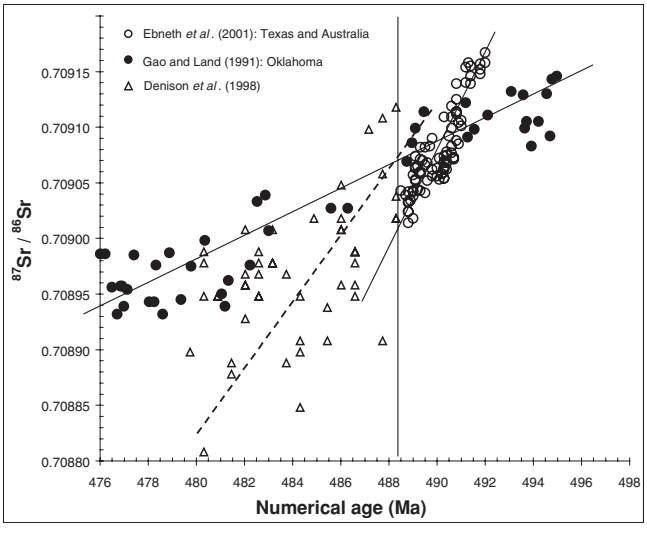

Figure 7.7 Data trends for the Cambrian–Ordovician boundary, showing the differences between authors.

interpreted as reflecting major geologic events (Shields *et al.*, 2003). The data of Qing *et al.* (1998) show a step around the Late–Middle Ordovician boundary of 0.708 041 to 0.708 698 over <1 myr, which must be a stratigraphic artifact. A lower, but still steep, decrease of $^{87}Sr/^{86}Sr$ starts in the late Darriwilian in the data of Shields *et al.* (2003); the decrease is less steep again for the data of Denison *et al.* (1998), probably because it starts in the early Darriwilian (equivalent). Where unusually steep rates of change of $^{87}Sr/^{86}Sr$ with time have been noted before, they have diminished with improved correlation, improved age models, or identification of altered samples. We have chosen to use Ebneth *et al.* (2001) for the Cambrian–Ordovician boundary interval and continue the Early and Middle Ordovician trend using the data of Denison *et al.* (1998), because that data relate to a few well-studied localities in the USA, and result in the least-steep decline through the Ordovician. The data of Shields *et al.* (2003) and Qing *et al.* (1998) supplement Denison *et al.* (1998) in the Late Ordovician.

Data gaps Finally, Fig. 7.2 reveals a paucity of reliable data for many intervals of time (the late Albian to Turonian, most of the Kimmeridgian and Berriasian, the Bajocian and Bathonian, much of the Permian and the Devonian, some of the Ordovician, and most of the Cambrian). This lack is reflected in the large (>0.000 015) half-width of the confidence interval on the mean for the LOWESS fit (Fig. 7.4); to reduce this uncertainty substantially will require some three–five accurate and precise $^{87}Sr/^{86}Sr$ values per biozone.